JOURNAL OF GUIDANCE, CONTROL, AND DYNAMICS
Vol. 31, No. 6, November–December 2008

Constrained Control Strategies to Improve Safety and Comfort on Aircraft

Domenico Famularo,* Davide Martino,† and Massimiliano Mattei‡
University of Reggio Calabria, 89060 Reggio Calabria, Italy

DOI: 10.2514/1.34426

The present paper explores the possibility of applying to an aircraft a novel constrained control methodology known as the command governor to improve flight safety and comfort. The proposed strategy is based on predictive control ideas and consists of the separate design of two control actions: an inner primal linear controller that guarantees the tracking of the controlled variables in the absence of constraints and an outer nonlinear static device (the command governor) that is compelled to modify, whenever necessary, the reference signals supplied to the inner controller by taking into account the limitations imposed by the aerodynamics, structures, actuators, and onboard comfort requirements. The reference signal modification is accomplished through an online constrained optimization procedure, which embodies the future plant evolution computed along a finite virtual time horizon. Two numerical examples are developed on a high-performance military aircraft and a small commercial aircraft.

Nomenclature

b, S	=	wing span, reference area
C_D, C_L, C_Y	=	drag, lift, and side force coefficients
C_l, C_m, C_n	=	roll, pitch, and yaw moment coefficients
$\bar{c}$	=	mean aerodynamic chord
g	=	gravity acceleration
h	=	altitude
I_x, I_y, I_z	=	momentum of inertia about X, Y, and Z (body axes)
I_{xz}	=	cross product of inertia
p, q, r	=	roll, pitch, and yaw rates
W, T, V	=	aircraft weight, thrust, and true air speed
α, β	=	angle of attack, sideslip
δ_{cr}, δ_{cl}	=	right and left canard deflection angles
δ_{cs}, δ_{cd}	=	symmetrical and differential canard deflection angles
δ_e, δ_a, δ_r	=	elevator, aileron and rudder deflection angles
δ_{th}	=	throttle command
δ_{tr}, δ_{tl}	=	right and left taileron deflection angles
δ_{ts}, δ_{td}	=	symmetrical and differential taileron deflection angles
μ_T	=	angle between the thrust direction and X body axis
ρ	=	air density, $\rho(h)$
ϕ, θ, ψ	=	roll, pitch, and yaw angles

I. Introduction

A KEY problem in flight control is the efficient treatment of constraints imposed on the normal operation of aircraft. These constraints are generated by saturating actuators, flight envelope limitations due to structures and aerodynamics, and other restrictions due to comfort and safety requirements [1].

Many different approaches have been investigated in the past to cope with these problems. Antiwindup (AW) and optimal AW/LQR and AW/H_2 are feedback control methodologies dealing with the presence of input constraints in an indirect manner [2–6]. Software rate limiters have been used to minimize the adverse effects due to the saturation of the actuators for both stable and unstable aircraft [7,8]. Other methods based on predictive control, genetic algorithms, and recovery guidance techniques have been investigated to deal with several kinds of aircraft limitations [9–11].

More recently, techniques based on invariant set arguments and predictive control ideas [12,13] have gained popularity due to their inherent capability to take the presence of constraints directly into account in the design phase. The control action is computed through the solution of a sequence of optimization problems based on the prediction of the plant state evolution. The objective is to jointly maximize the control performance and enforce the satisfaction of the prescribed constraints. The interest in such methodologies has been growing in the last decade [14,15] due to the availability of fast computing units (real-time systems, Neuro–Fuzzy, soft computing devices, etc.).

This paper deals with predictive control methodologies that are mainly devoted to constraint fulfillment, leaving to traditional regulation frameworks the performance achievement (set point tracking, disturbance rejection, robustness issues, etc.). Such a family of control strategies is known in the literature as the command governor (CG) approach. The CG is a nonlinear device that is added to a primal inner controller designed so as to exhibit stability and tracking performance in the absence of constraints. At each discrete time instant, t_k, the CG outer device computes a modified reference command that, if applied from t_k onward, does not produce constraint violations. Such a modified reference command is computed to minimize its distance from the actual desired reference signal according to an online constrained optimization over a receding horizon finite time interval.

Many mature assessments of the CG state of the art for linear systems can be found in [16–23]; specific results on the CG strategy for nonlinear systems are reported in [24,25].

The objective of this paper is to explore the possibility of applying the CG framework to improve safety and comfort on aircraft with a negligible impact on the primal flight control performance. Two numerical examples are considered to show the effectiveness of the proposed strategy. The first example is an application to a high incidence research model (HIRM) of a twin-engine fighter aircraft first used in the FM-AG08-GARTEUR research activities [26,27].

Received 4 September 2007; revision received 30 November 2007; accepted for publication 2 January 2008.

*Associate Professor, Department of Computer Science, Mathematics, Electronics and Transport, Via Graziella, Loc. Feo di Vito; domenico.famularo@unirc.it. Member AIAA.

†Ph.D. Student, Department of Computer Science, Mathematics, Electronics and Transport, Via Graziella, Loc. Feo di Vito; davide.martino@unirc.it.

‡Professor, Department of Computer Science, Mathematics, Electronics and Transport, Via Graziella, Loc. Feo di Vito; massimiliano.mattei@unirc.it. Member AIAA.

The second example considers a small commercial aircraft [28] (SCA) of the general aviation.

The paper is organized as follows. In Sec. II, the aircraft mathematical model is briefly recalled and the primal controller structure is outlined. In Sec. III, the CG approach is described from a theoretical point of view and some computational issues are also discussed. Finally, in Sec. IV, some numerical results on the two selected aircraft are provided. The benefits of the CG are also discussed in this section.

II. Problem Formulation, Mathematical Model, and Primal Controller Structure

The aircraft represents a significant example of a system inherently subject to input/state constraints. Modern flight control systems are required to guarantee high performance, pushing the aircraft toward its operative limitations [1].

The restrictions arising in flight control problems are mainly due to aerodynamics, structures, actuators, and safety and comfort requirements. They can be translated into a set of constraints on aircraft model variables such as the angles of attack and sideslip, the altitude, the accelerations, the speed and the loading factors, the deflection angles of the control surfaces, the throttle command amplitudes, the angular rates, etc.

As stated in the introduction, a constrained control problem solved by means of the CG framework is viewed as a two-step procedure. First, a primal inner control loop is designed so as to achieve tracking capabilities in the absence of constraints. Then, the CG outer device is superimposed to guarantee the satisfaction of the aforementioned constraints. In this section, we will briefly recall some aspects related to the aircraft modeling and the design of the inner control loop.

A. Aircraft Model

In the so-called polar form [1], the six-degree-of-freedom mathematical model of an aircraft has the following structure:

$$\begin{aligned} W\dot{V} &= T\cos(\alpha+\mu_T)\cos\beta - \tfrac{1}{2}\rho V^2 S C_D \\ &\quad + Wg(-\cos\alpha\cos\beta\sin\theta + \sin\beta\sin\phi\cos\theta \\ &\quad + \sin\alpha\cos\beta\cos\phi\cos\theta) \end{aligned} \tag{1}$$

$$\begin{aligned} WV\dot{\alpha}\cos\beta &= -T\sin(\alpha+\mu_T) - \tfrac{1}{2}\rho V^2 S C_L + WVq \\ &\quad + Wg(\sin\alpha\sin\theta + \cos\alpha\cos\phi\cos\theta) \end{aligned} \tag{2}$$

$$\begin{aligned} VW\dot{\beta} &= -T\cos(\alpha+\mu_T)\sin\beta + \tfrac{1}{2}\rho V^2 S C_Y - WVr \\ &\quad + Wg(\cos\alpha\sin\beta\sin\theta + \cos\beta\sin\phi\cos\theta \\ &\quad - \sin\alpha\sin\beta\cos\phi\cos\theta) \end{aligned} \tag{3}$$

$$\dot{p}I_x - \dot{r}I_{xz} + qr(I_z - I_y) - pqI_{xz} = \tfrac{1}{2}\rho V^2 S b C_l \tag{4}$$

$$\dot{q}I_y + rp(I_x - I_z) + (p^2 - r^2)I_{xz} = \tfrac{1}{2}\rho V^2 S \bar{c} C_m \tag{5}$$

$$-\dot{p}I_{xz} + \dot{r}I_z + pq(I_y - I_x) + qrI_{xz} = \tfrac{1}{2}\rho V^2 S b C_n \tag{6}$$

$$\dot{\phi} = p + q\tan\theta\sin\phi + r\tan\theta\cos\phi \tag{7}$$

$$\dot{\theta} = q\cos\phi - r\sin\phi \tag{8}$$

$$\dot{\psi} = r\cos\phi\sec\theta + q\sin\phi\sec\theta \tag{9}$$

The aerodynamics coefficients C_D, C_L, C_Y, C_l, C_m, and C_n can be expressed as a function of the state variables V, α, β, ϕ, θ, ψ, p, q, r, and h and of the input variables δ_e (δ_{cs}, δ_{ts}), δ_a (δ_{cd}, δ_{td}), and δ_r for the civil (military) aircraft under consideration in this study. The thrust is a nonlinear function of the state and the input variable δ_{th}.

If an external wind acts as an exogenous disturbance, the speed V, angle of attack α, and sideslip β are nonlinear functions of the wind velocity vector $[u_{wind}, v_{wind}, w_{wind}]^T$. Here, the external atmospheric turbulence is generated with a Dryden continuous-time turbulence model, whereas a windshear model is simulated on the basis of the MIL-F-8785C military specification.

B. Primal Controller Design

The primal controller adopted for the aircraft is a standard optimal multivariable proportional plus integral (PI) controller designed with respect to a linear time-invariant model of the aircraft obtained by linearizing equations (1–9) around a fixed operating point. It has been proven in [29,30] that, in spite of its low order, this kind of controller, whose structure is shown in Fig. 1, can be regarded as a valid option with respect to more complex multivariable controller structures. Moreover, the primal control law design phase represents a minor detail aspect in this paper that is mainly devoted to analyzing the performance of the CG device.

Starting from Eqs. (1–9), we define with 1) $\hat{x} := [V, \alpha, \beta, \phi, \theta, \psi, p, q, r]^T$, the plant state; 2) $u := [\delta_e, (\delta_{cs}, \delta_{ts})\delta_a, (\delta_{cd}, \delta_{td})\delta_r, \delta_{th}]^T$, the control input vector for the civil (military) aircraft under consideration; 3) $\hat{d} := [u_{wind}, v_{wind}, w_{wind}]^T$, the disturbance vector; 4) z, the state vector affected by the disturbance; and 5) y, the controlled output vector.

A linearized model computed in the neighborhood of a certain flight condition has the following structure:

$$\begin{cases} \dot{\hat{x}} = A\hat{x} + \hat{B}_1\hat{d} + B_2 u \\ z = \hat{x} + \hat{D}_1\hat{d} \end{cases} \tag{10}$$

By defining the new state and disturbance vectors as follows

$$x := \hat{x} + \hat{D}_1\hat{d} \qquad d := [\,\hat{d}^T \quad \dot{\hat{d}}^T\,]^T$$

we have

$$\begin{cases} \dot{x} = Ax + B_1 d + B_2 u \\ y = C_r x \end{cases} \tag{11}$$

with $B_1 = [\,(\hat{B}_1 - \hat{A}\hat{D}_1) \quad \hat{D}_1\,]$.

To obtain a guaranteed level of tracking performance, the plant equation (11) is augmented with a multivariable integrator (see Fig. 1), and the control action is derived according to a standard linear quadratic regulator (LQR) strategy. The controller parameters are so obtained by minimizing the quadratic performance index:

$$\begin{aligned} &\int_0^\infty (x_a^T Q_a x_a + u^T R_a u)\,\mathrm{d}t \\ &\text{s.t. } \dot{x}_a = A_a x_a + B_{a_1} d + B_{a_2} u + B_{a_3} r \end{aligned} \tag{12}$$

where $Q_a \geq 0$ and $R_a > 0$ are two suitable state and input symmetric weighting matrices, $x_a = [\,x^T \quad x_i^T\,]^T$ is the augmented state vector including the plant and the integrator state variables, r is the reference signal, and

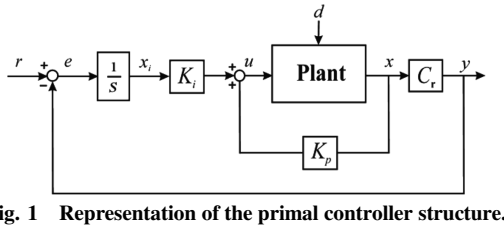

Fig. 1 Representation of the primal controller structure.

$$A_a = \begin{pmatrix} A & 0 \\ -C_r & 0 \end{pmatrix}; \quad B_{a1} = \begin{pmatrix} B_1 \\ 0 \end{pmatrix}; \quad B_{a2} = \begin{pmatrix} B_2 \\ 0 \end{pmatrix}; \quad B_{a_3} = \begin{pmatrix} 0 \\ I_{n_y} \end{pmatrix}$$

(A_a, B_{a2}) and $(A_a, \sqrt{Q_a})$ are a stabilizable and a detectable pair, respectively.

According to the scheme shown in Fig. 1, a control action in the form

$$u = K_p x + K_i x_i \tag{13}$$

is computed. The terms K_p and K_i denote the proportional and integral gain matrices that are obtained by partitioning the state feedback matrix gain $K_a = [\,K_p \quad K_i\,]$ obtained from the solution of the LQR problem (12).

In what follows, some preliminary details regarding the design procedure of the CG device that is devoted to constraint satisfaction will be provided. It is worth noting that, although the primal controller design is carried out in a continuous time framework, the design and implementation of the outer CG control loop is obtained within a discrete time sampled data scheme. A zero order hold algorithm is used to discretize the aircraft linearized model including the primal control action (plant shown in Fig. 1).

III. Command Governor Strategy

Limitations on the plant state evolution and/or the control input can lead to performance degradation, windup phenomena, and even instability. To cope with these problems, the command governor is a methodology mainly devoted to enforcing all of the prescribed constraints by properly modifying the reference signal supplied to the precompensated plant.

A. Mathematical Formulation

In its most common formulation [16–22], according to the scheme depicted in Fig. 2, the CG approach takes into consideration a discrete time, precompensated time-invariant plant:

$$\begin{cases} x(t_{k+1}) = \Phi x(t_k) + G\vartheta(t_k) + G_d d(t_k) \\ y(t_k) = H_y x(t_k) \\ c(t_k) = H_c x(t_k) + L\vartheta(t_k) + L_d d(t_k) \end{cases} \tag{14}$$

where $t_k = t_0 + kT_s$, $k \in \mathbb{Z}_{0+}$, and t_0, T_s are the initial time instant and the sampling interval respectively; $x(t_k) \in \mathbb{R}^{n_x}$ is the state vector including the plant and the primal controller states; and $\vartheta(t_k) \in \mathbb{R}^{n_r}$ is the command input vector that would coincide with the reference signal $r(t_k) \in \mathbb{R}^{n_r}$ if no constraints were present. $d(t_k) \in \mathbb{R}^{n_d}$ is an exogenous disturbance vector belonging to a convex and compact set,

$$\mathcal{D} = \{d \in \mathbb{R}^{n_d} \colon Ud \le \bar{h}\} \tag{15}$$

where $U \in \mathbb{R}^{n_u \times n_d}$ $(n_u \ge n_d)$ is a full column rank matrix, and $\bar{h} = [\,\bar{h}_1 \quad \bar{h}_2 \cdots \bar{h}_{n_u}\,]^T \in \mathbb{R}^{n_u}$ is a vector of nonnegative constraints $(\bar{h}_p \ge 0,\ p = 1, \ldots, n_u)$. $y(t_k) \in \mathbb{R}^{n_r}$ is the controlled output vector (which is required to track $r(t_k)$), and $c(t_k) \in \mathbb{R}^{n_c}$ is the vector to be constrained belonging to a convex and compact set

$$C = \{c \in \mathbb{R}^{n_c} \colon Tc \le f\} \tag{16}$$

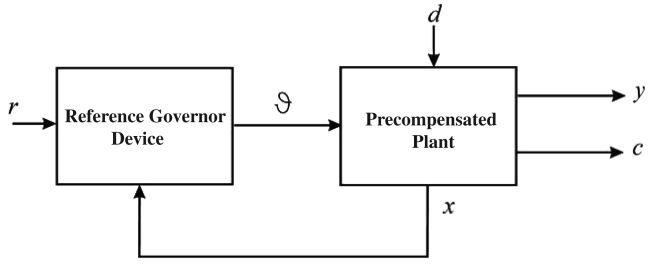

Fig. 2 Control scheme with the command governor.

where $T \in \mathbb{R}^{n_t \times n_c}$, $n_t \ge n_c$, is a full column rank matrix, and $f \in \mathbb{R}^{n_t}$ is a constant vector of constraints.

Under the assumptions that the system equation (14) is asymptotically stable and offset free (i.e., $H_y(I_{n_x} - \Phi)^{-1}G = I_{n_r}$), the CG design problem consists of finding, at each time t_k, a command $\vartheta(t_k) = \underline{\vartheta}(x(t_k), r(t_k))$ as a memoryless function of the current state and reference signal, which is the best approximation of $r(t_k)$ at time t_k under all possible disturbance sequences within $\mathcal{D}$ and compatible with the constraint set $\mathcal{C}$ (i.e., $d(t_{k+h}) \in \mathcal{D}$, $c(t_{k+h}) \in \mathcal{C}$, $\forall\ h \ge 0$).

To propose a workable numerical procedure, the role of external disturbances and commands with respect to the prescribed constraint set equation(16) must be clarified.

The disturbance effect is taken into account using a P-difference [31,32] argument. The P-difference (also known as Minkowski difference) operation, indicated with the symbol $\sim$, is defined as follows:

$$\mathcal{A} \sim \mathcal{B} = \{a \in \mathbb{R}^n :\ a + b \in \mathcal{A}, \quad \forall\ b \in \mathcal{B}\}$$

Starting from a compact constraint set $\mathcal{C}$, the following sequence of sets $\mathcal{C}_h$, $h = 0, 1, \ldots$ is defined

$$\mathcal{C}_0 := \mathcal{C} \sim L_d\mathcal{D}, \qquad \mathcal{C}_h := \mathcal{C} \sim L_d\mathcal{D} \sim \cdots \sim H_c\Phi^{h-1}G_d\mathcal{D}, \qquad h \ge 1$$

which can be obtained by means of the following recursion:

$$\mathcal{C}_0 := \mathcal{C} \sim L_d\mathcal{D}, \ldots, \mathcal{C}_h := \mathcal{C}_{h-1} \sim H_c\Phi^{h-1}G_d\mathcal{D} \tag{17}$$

All of the elements $\mathcal{C}_h$, $h = 0, 1, \ldots$ are compact and satisfy $\mathcal{C}_h \subseteq \mathcal{C}_{h-1}$. As a consequence, there exists the so-called maximal approximation [31,32],

$$\mathcal{C}_\infty := \bigcap_{i=0}^{\infty} C_i \tag{18}$$

which is still a nonempty convex and compact set.

The set $\mathcal{C}_h$ turns out to be a suitable restriction of $\mathcal{C}$ [32] such that, if the "disturbance-free" component of $c(t_k)$, depending on the initial state and the input time sequence, belongs to $\mathcal{C}_h$, then $c(t_k)$ belongs to $\mathcal{C}$, for all $k \le h$ in the presence of disturbances.

The commands are instead considered by defining the convex and closed set $\mathcal{W}^\xi$ (assumed nonempty), which characterizes all constant inputs $\omega \in \mathbb{R}^{n_r}$ whose corresponding disturbance-free steady-state solutions of Eq. (14), $\bar{c}_\omega = H_c(I_{n_x} - \Phi)^{-1}G\omega + L\omega$, satisfy the constraints within a prescribed tolerance ξ.

Once the role of disturbances and commands is clarified, the CG strategy consists of computing, at each time step t_k, a constant virtual command, $\omega \in \mathcal{W}^\xi$, such that the corresponding disturbance-free evolution from the measured state $x(t_k)$,

$$\bar{c}(t_{k+h}, x(t_k), \omega) = H_c\left(\Phi^h x(t_k) + \sum_{i=0}^{h-1} \Phi^{h-i-1}G\omega\right) + L\omega$$

belongs to the restricted constraint set sequence $\mathcal{C}_h$, $\forall\ h > k$ (Eq. (17) accounting for disturbance effects), and its distance from the reference $r(t_k)$ is minimal. Such a command is applied to the plant in the time interval $[t_k, t_{k+1}[$, and the procedure is repeated at the next time t_{k+1} on the basis of the new measured state $x(t_{k+1})$.

Consequently, if we denote with $\mathcal{V}(x(t_k)) \subset \mathcal{W}^\xi$ the set of all constant commands $\omega \in \mathcal{W}^\xi$, whose corresponding c evolutions starting from an initial condition $x(t_k)$, at time t_k, also satisfy the constraints during the transient period (i.e., $\mathcal{V}(x(t_k)) := \{\omega \in \mathcal{W}^\xi :\ \bar{c}(t_{k+h}, x(t_k), \omega) \in \mathcal{C}_h,\ \forall\ h > 0\}$, and provided that $\mathcal{V}(x(t_k))$ is nonempty, closed and convex for all t_k, the CG command is the solution of the following constrained optimization problem:

$$\vartheta(t_k) = \arg \min_{\omega \in \mathcal{V}(x(t_k))} J(r(t_k), \omega) \tag{19}$$

where

$$J(r(t_k),\omega) := \|\omega - r(t_k)\|_{\Psi}^2 \tag{20}$$

where $\|x\|_{\Psi}^2 := x^T\Psi x$ is a weighted norm with Ψ a positive definite symmetric matrix.

In other words, the minimizer equation (19) represents the best approximation of the reference signal $r(t_k)$, which, if constantly applied from t_k onward to system equation (14), would never produce a constraint violation.

The implementation of the CG strategy requires a finite-time computable way to solve the optimization problem (19). To overcome the difficulties due to the infinite number of steps/constraints in the definition of $\mathcal{V}(x(t_k))$, it has been shown in [17,33] that $\mathcal{V}(x(t_k))$ can be finitely determined.

In fact, there exists an integer k^* such that, if $\bar{c}(t_{k+h}, x(t_k), \omega) \in \mathcal{C}_h,\ h \in \{0, 1, \ldots, k^*\}$, then $\bar{c}(t_{k+h}, x(t_k), \omega) \in \mathcal{C}_h,\ \forall\ h \geq 0$. The horizon length value k^* can be obtained according to the algorithm proposed in [33], which is based on the solution of the following optimization problem [34]:

$$\begin{aligned} G_k(j) = &\max_{x\in\mathbb{R}^{n_x},\omega\in\mathcal{W}^{\xi}} T_j\bar{c}(t_k, x, \omega) - f_j^k \\ &\text{subject to } T_j\bar{c}(t_i, x, \omega) \leq f_j^i, \qquad i = 0, \ldots, k-1 \end{aligned} \tag{21}$$

where $T_j,\ j = 1, \ldots, n_t$ denotes the jth row of matrix T and f_j^i, $i = 0, \ldots, k-1$ have the following expression:

$$\begin{aligned} f_j^0 &= f_i - \sup_{d\in\mathcal{D}} T_j L_d d \qquad f_j^1 = f_i^0 - \sup_{d\in\mathcal{D}} T_j H_c G_d d \\ f_j^{k-1} &= f_j^{k-2} - \sup_{d\in\mathcal{D}} T_j H_c \Phi^{k-1-j} G_d d \end{aligned} \tag{22}$$

Equation (22) represents a correction to the constraint vector, based on the P-difference operator between sets defined in Eq. (17), which allows us to take into account the presence of disturbances.

The algorithm to derive the finite constraint horizon k^* is the following:

Step 1: $k = 1$.

Step 2: Find $G_k(j)$ solving problem (21) $\forall\ j = 1, \ldots, n_t$.

Step 3: If $G_k(j) \leq 0,\ \forall\ j = 1, \ldots, n_t$; then, set $k^* = k$ and stop; else, if $k = k + 1$, go to *Step 2*; end.

With the application of this algorithm that can be performed offline, the optimization problem (21) is converted into a quadratic programming (QP) problem with a finite number of constraints to be solved online, that is,

$$\begin{aligned} \vartheta(t_k) := &\min_{\omega\in\mathcal{W}^{\xi}} J(r(t_k),\omega) \quad \text{subject to } TH_c\Phi^h x(t_k) \\ &+ T\sum_{i=0}^{h-1}\Phi^{i-h-1}G\omega + TL\omega \leq f^h, \qquad h = 0, \ldots, k^* \end{aligned} \tag{23}$$

In the case that system equation (14) satisfies the offset-free and asymptotic stability assumptions and that $\mathcal{V}(x(t_k))$ is nonempty, the minimum for problem (23) uniquely exists at each time. Moreover, $\mathcal{V}(x(t_k))$ nonempty implies $\mathcal{V}(x(t_{k+h}))$ nonempty for all h along the trajectories generated by the CG command (viability property). Finally, the constraints are always fulfilled and the overall closed loop system is asymptotically stable.

In particular, whenever $r(t_k) \equiv r$, $\vartheta(t_k)$ monotonically converges in finite time to either r or its best admissible approximation compatible with constraints

$$\hat{r} := \arg\min_{\omega\in\mathcal{W}^{\xi}} J(r,\omega)$$

Consequently, by the offset-free condition

$$\lim_{t_k\to+\infty} \bar{y}(t_k) = \hat{r}$$

where $\bar{y}(t_k)$ denotes the disturbance-free component of the plant output.

B. Computational Aspects

As for the computational aspects of the proposed technique, it is worth pointing out that the off-line problem (21) represents a linear programming problem, which can be solved using standard simplex algorithms, whereas problem (23), which has to be solved online, is a convex QP problem that can be solved through any common solver embedded in any main commercial optimization and control software package.

As it will be shown in the next section, QP solvers provide a solution that can be obtained "fast enough" to be online implemented for our purposes. However, we cannot theoretically assure that a solution is given within a sampling time interval. In the event that, at a given time instant, the CG computation time of the command $\vartheta(t_k)$ exceeds the control system sampling interval, it is possible to resort to a nonoptimal, though feasible and compatible with the constraints, strategy, that is, $\vartheta(t_k) \leftarrow \bar{\vartheta}(t_{k-1})$, where $\bar{\vartheta}(t_{k-1})$ denotes the CG command computed at the time instant previous to t_k. This strategy is justified from a theoretical point of view by the viability property mentioned in the previous subsection and discussed in [17,22,31,33].

Some guidelines on the computation of the set $\mathcal{W}^{\xi}$ are also useful because this is a key ingredient in the numerical implementation of the CG.

First of all, the set $\mathcal{C}_\infty$, which is necessary to compute $\mathcal{W}^{\xi}$, can be numerically approximated with a convenient $\mathcal{C}_\infty^a(\varepsilon)$ such that

$$\mathcal{C}_\infty^a(\varepsilon) \subset \mathcal{C}_\infty \subset \mathcal{C}_\infty^a(\varepsilon) + \mathcal{B}_\varepsilon \tag{24}$$

where $\mathcal{B}_\varepsilon$ represents a ball of radius ε (safety level) centered at the origin. Such a set is computable in a finite number of steps. In fact, it can be shown that

$$\mathcal{C}_\infty = \mathcal{C}_k \sim \left(\sum_{i=k}^{\infty} H_c\Phi^i G_d\mathcal{D}\right) \tag{25}$$

The stability of matrix Φ implies the existence of two positive constants, M and $\lambda \in (0,1)$, such that $\|\Phi^k\|_2 \leq M\lambda^k$, whereas the boundedness of $\mathcal{D}$ implies the existence of

$$d_{\max} := \max_{d\in\mathcal{D}} \|d\|_2$$

As a consequence, for each $\varepsilon > 0$, there exists an index $k_\varepsilon > 0$ such that

$$\sum_{i=k}^{\infty} H_c\Phi^i G_d\mathcal{D} \subset \mathcal{B}_\varepsilon \quad \text{for all } k > k_\varepsilon \tag{26}$$

Once the prescribed tolerance is fixed and M, λ, and $d_{\max}$ are determined, due to the following inequality

$$d_{\max}\bar{\sigma}(H_c)\bar{\sigma}(G_d)M\sum_{i=k_\varepsilon}^{\infty}\lambda^i \leq \varepsilon \tag{27}$$

And the value of k_ε can be computed as [35]

$$k_\varepsilon = \frac{\ell_n(\varepsilon) + \ell_n(1-\lambda) - \ell_n(\bar{\sigma}(H_c)\bar{\sigma}(G_d)Md_{\max})}{\ell_n(\lambda)} \tag{28}$$

Now if we also consider the tolerance margin ξ on the constraint fulfillment, we have the following approximation of $\mathcal{C}_\infty$: $\mathcal{C}_\infty^{a\xi}(\varepsilon) = (\mathcal{C}_{k_\varepsilon} \sim \mathcal{B}_\varepsilon) \sim \mathcal{B}_\xi$ that can be used to compute $\mathcal{W}^{\xi}$ by solving the problem of determining all commands $\omega \in \mathbb{R}^{n_r}$ such that $\bar{c}_\omega \in \mathcal{C}_\infty^{a\xi}(\varepsilon)$. Finally, we have $\mathcal{W}^{\xi}$ defined as

$$\begin{aligned} \mathcal{W}^{\xi} = \{&\omega \in \mathbb{R}^{n_r} :\ TH_c(I_{n_x} - \Phi)^{-1}G\omega + TL\omega \\ &\leq f^{k_\varepsilon} - (\xi + \varepsilon)\sqrt{T_j^T T_j} \qquad j = 1, \ldots, n_t\} \end{aligned} \tag{29}$$

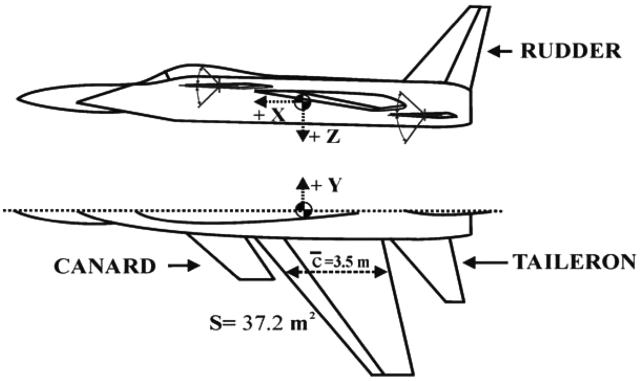

Fig. 3 High-incidence research model.

IV. Application of CG Strategy to Civil Small Commercial and Fighter Aircraft

In this section, the application of the CG strategy presented in Sec. III to the flight control problem is discussed through two numerical examples: the former takes into account a high-performance fighter aircraft and the latter considers a small commercial aircraft of general aviation.

For the sake of clarity, the performance of the primal multivariable PI controller will be discussed first, and then the results compared with those achieved using the CG device. All the simulation experiments have been done within the MATLAB/Simulink environment.

A. Fighter Aircraft Application Example

The high incidence research model (HIRM) is a mathematical model of a generic fighter aircraft originally developed by the Defence and Evaluation Research Agency, Bedford, United Kingdom. The HIRM is based on aerodynamic data obtained from wind-tunnel experiments and flight testing of an unpowered and scaled drop model. The model has been built to investigate flight conditions with high angle-of-attack values (between -50 and 120 deg) and a wide sideslip range ($[-50, +50$ deg$]$). Conversely, the compressibility effects resulting from high subsonic speeds have not been taken into consideration. The unconventional aircraft configuration, with both a canard and tailplane plus an elongated nose, is shown in Fig. 3. The aircraft is basically stable; however, there are combinations of the angle of attack and the control surface deflections that cause the aircraft to become longitudinally and/or laterally unstable. Engine, actuator, and sensor dynamics models have been added within the FM-AG-08-GARTEUR research activities [26,27] to create a significant nonlinear simulation model of a twin-engined, modern fighter aircraft. A MATLAB/Simulink simulator was also developed during the FM-AG08 project. Table 1 provides the main parameters of the HIRM aircraft.

Table 1 HIRM main parameters, constraints, and equilibrium conditions

$I_x = 24,550$ kg m^2		
$I_y = 163,280$ kg m^2		
$I_z = 183,100$ kg m^2		
$I_{xz} = 3120$ kg m^2		
$S = 37.2$ m^2		
$W = 15,300$ kg		
$\bar{c} = 3.5$ m		
Variable	Min.	Max.
δ_{tl}, δ_{tr}	-0.69 rad	0.17 rad
δ_{cr}, δ_{cr}	-0.34 rad	0.17 rad
δ_r	-0.52 rad	0.52 rad
$d\delta_{tl}/dt, d\delta_{tr}/dt$	-1.39 rad/s	1.39 rad/s
$d\delta_{cl}/dt, d\delta_{cr}/dt, d\delta_r/dt$	-1.39 rad/s	1.39 rad/s
p	-2.6 rad/s	2.6 rad/s
α	-0.17 rad	0.52 rad
β	-0.17 rad	0.17 rad
Equilibrium flight conditions at $h = 1500$ m, Mach $= 0.3$		
δ_{ts}	-0.035 rad	
$\delta_{cd}, \delta_{cs}, \delta_{td}, \delta_r$	0 rad	
δ_{th}	56%	
p, q, r	0 rad/s	
V	100 m/s	
α, θ	0.31 rad	
ϕ, β	0 rad	

1. Flight Control Problem and Primal Controller

The PI regulator used for the inner primal control loop (see Fig. 1) has been designed with respect to a wing leveled straight flight condition at Mach $= 0.3$ and an altitude of 1500 m (see Table 1 for the definition of the equilibrium). Roll and pitch rates together with the angle of sideslip have been chosen as controlled variables. The throttle command has been assumed to be constant during maneuvers.

The simulation results obtained on the nonlinear model of the aircraft [27] equipped with the PI controller are analyzed in the presence of the following conditions: a pilot demand of ± 2.6 rad/s on p (doublet, 0.3 s negative, and 0.3 s positive), a pilot demand of ± 1.0 rad/s on q (doublet, 0.3 s negative, and 0.3 s positive), a pilot demand of 0 rad on β, and severe atmospheric turbulence generated with a Dryden model (maximum wind speed 12 m/s and a standard deviation of 3 m/s).

Figure 4 provides a comparison between the reference trajectories (solid line) and the related controlled outputs in the presence of the primal controller in the absence of constraints acting on the aircraft.

The angular rates exhibit a fast response and the angle of sideslip breaks through its allowed excursion range because of the strong disturbance acting on the plant. Undesirable effects due to the aggressive pilot demand can be observed in Figs. 5 and 6, in which the time-behavior of the control variables is reported. It happens that the values of the taileron and canard deflection angles required by the linear controller are violating their prescribed limits on the amplitudes and rates. Also, the angle of attack is forced out of the admissibility range.

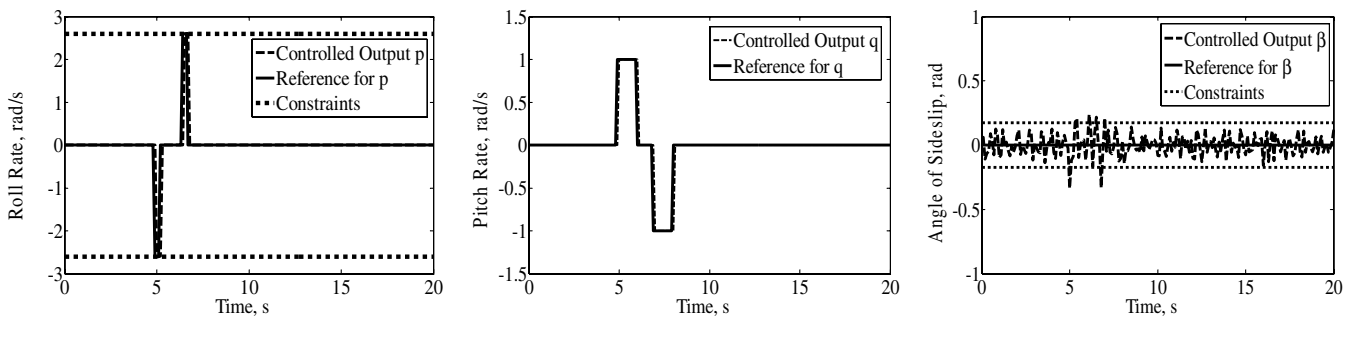

a) b) c)

Fig. 4 HIRM model. Primal PI controller performance. Reference trajectories for the p, q, and β variables (solid line) and controlled outputs (dashed line). No constraints, no CG action.

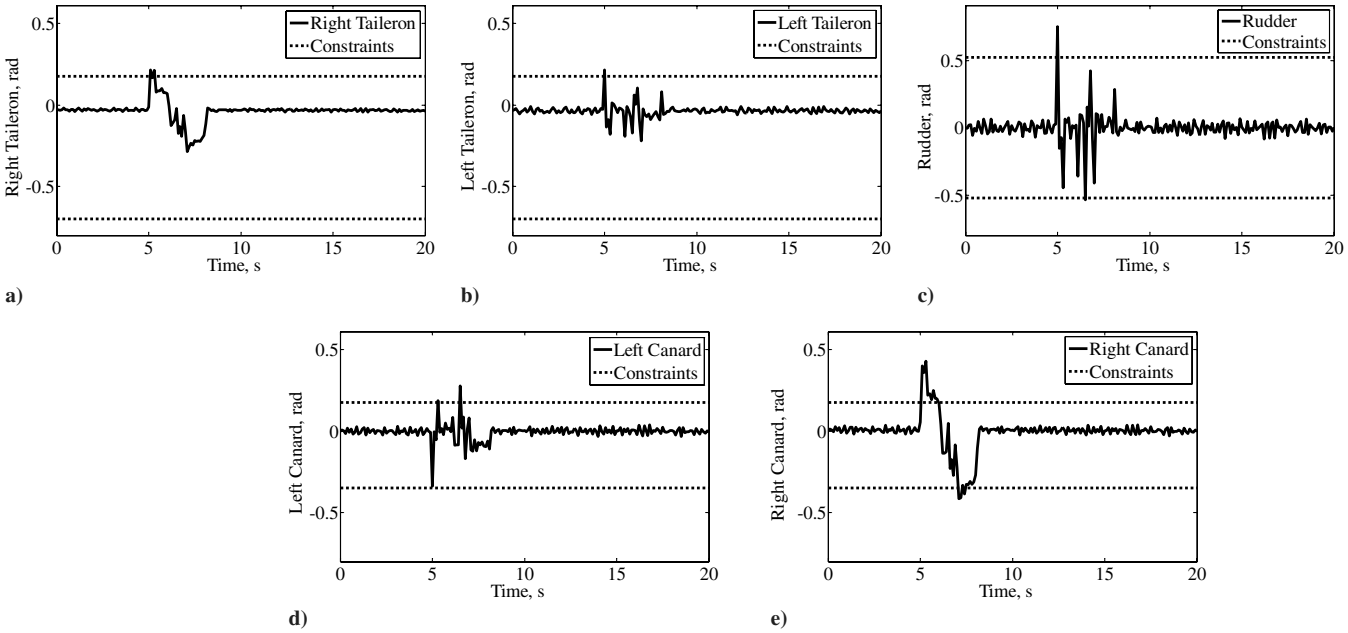

Fig. 5 HIRM model. Time behavior of the control surface deflections (Primal PI controller, no constraints, no CG action).

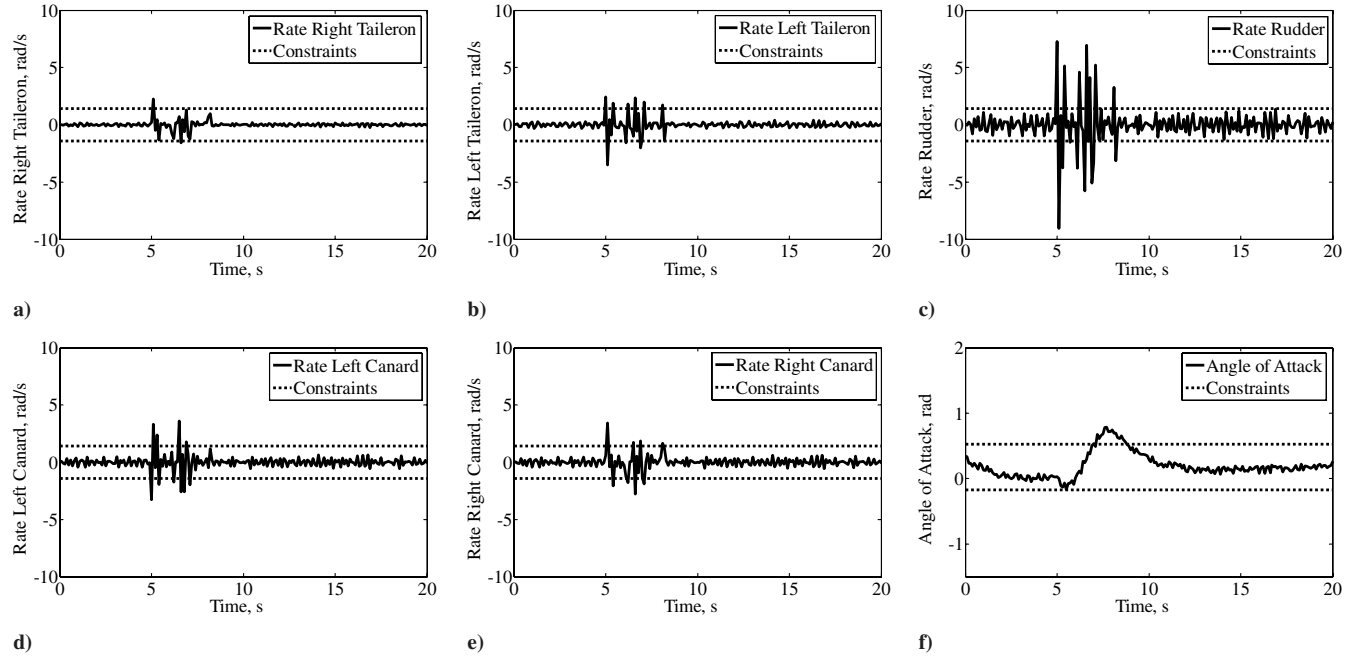

Fig. 6 HIRM model. Time behavior of the angular rates of the control surface deflections and of the angle of attack (Primal PI controller, no constraints, no CG action).

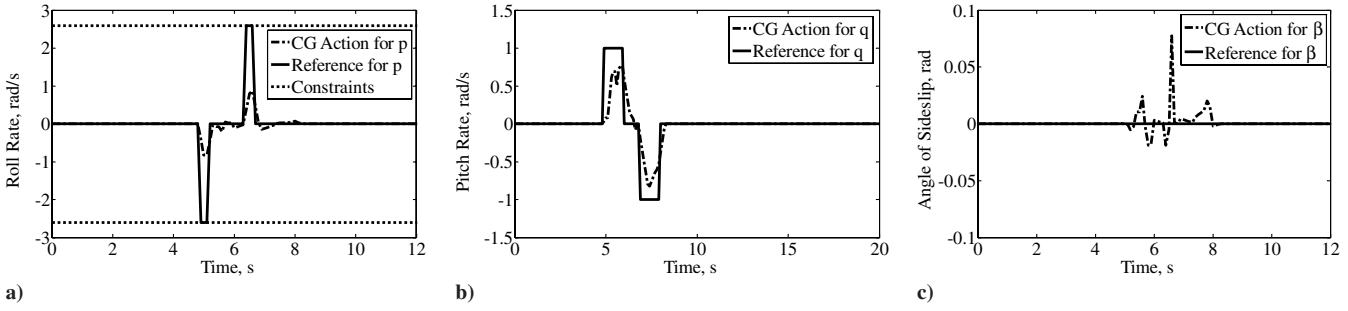

Fig. 7 HIRM model. Comparison between the pilot reference signals (solid line) and their modifications provided by the CG device (dashed line).

It is worth noting that, although the primal controller is designed by assuming as control inputs the symmetric and differential deflections of both the canard and taileron to clearly distinguish between lateral and longitudinal actions, the physical constraints are imposed on the left and right deflections as reported in Table 1. The relationship between the aforementioned variable is $\delta_{t(c)r} = \delta_{t(c)s} + \delta_{t(c)d}$, $\delta_{t(c)l} = \delta_{t(c)s} - \delta_{t(c)d}$ for the taileron (canard).

A key remark is that, with the present primal controller, if all the physical constraints on the actuators reported in Table 1 are taken into account in the simulation, a fatal unstable behavior of the aircraft occurs in the presence of the aforementioned conditions.

2. Performance Achieved with CG Device

To recover stability, to guarantee satisfactory tracking performance, and to reject atmospheric disturbance, enforcing the prescribed limitations provided in Table 1, the fighter aircraft has been equipped with a CG device.

The value of the finite time $k^* = 28$ was computed solving problem (21) offline. Set $\mathcal{C}$ can be readily obtained from the constraints reported in Table 1, whereas set $\mathcal{D}$ is determined by the assumption that the external wind velocity vector has components within the interval $[-15, +15]$ m/s, with time derivatives within the interval $[-150, +150]$ m/s^2. Problem (23) is solved online by means of the QP solver of Matlab.

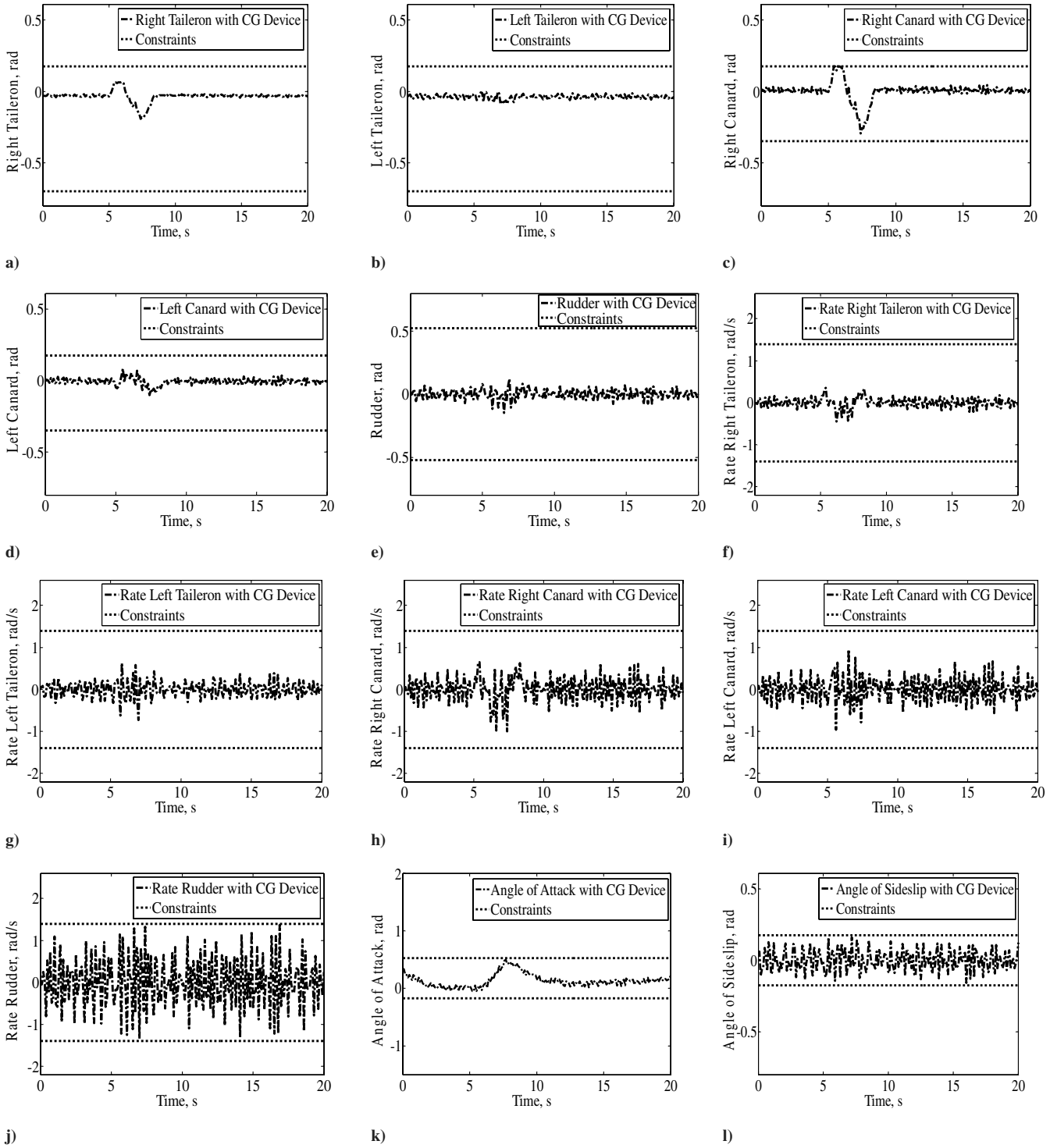

Fig. 8 HIRM model. Time behavior of the constrained outputs of the aircraft equipped with the CG device.

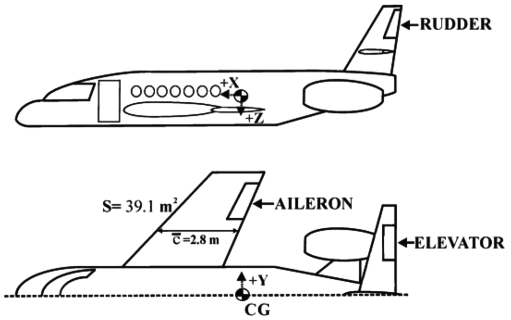

Fig. 9 Scheme of the SCA under consideration.

Figure 7 shows the comparison between the original pilot demands and the reference set points modified by the CG action. The modified doublets for p and q (dashed line) exhibit a reduced amplitude and a sort of filtered time behavior. The β reference trajectory is noticeably modified by the CG device to counteract the presence of turbulence. Figure 8 shows the time behavior of the main constrained outputs in the presence of a CG action. All the variables are forced to stay within their required bounds.

B. Small Commercial Civil Aircraft Application Example

The general aviation aircraft considered in this second application example is the SCA considered during the Affordable Digital Flight Control System, Phase II (ADFCSII) project [28]. The main characteristics of such an aircraft are summarized in Table 2 and the configuration is shown in Fig. 9. The simulation tool used in this study was developed during the ADFCSII research project under the Matlab/Simulink environment.

1. *Flight Control Problem and Primal Controller*

For the small commercial aircraft under consideration, the PI regulator discussed in Sec. II.B has been designed with respect to a wing leveled straight flight condition at Mach $= 0.6$ and an altitude of 7500 m (see Table 2 for details). ϕ, θ, and β have been chosen as controlled variables.

The simulation results obtained on the nonlinear model of the aircraft [28] equipped with the PI controller are analyzed in the presence of the following conditions: a pilot demand of 0.2 rad on ϕ (4 s time window), a pilot demand of 0.7 rad on θ (5 s time window), a pilot demand of 0.17 rad on β (5 s time window), and severe turbulence (maximum wind speed 10 m/s and a standard deviation of about 2 m/s).

Figure 10 shows the nominal performance obtained in the presence of the PI control action but in the absence of active constraints on the system. This condition has been achieved by scaling the aforementioned pilot set points to values compatible with the constraints.

Table 2 SCA main parameters, constraints, and equilibrium conditions

$I_x = 74,500$ kg m^2		
$I_y = 243,140$ kg m^2		
$I_z = 332,730$ kg m^2		
$I_{xz} = 12,660$ kg m^2		
$W = 17,100$ kg		
$S = 39.1$ m^2		
$\bar{c} = 2.8$ m		
Variable	Min.	Max.
δ_e	−0.48 rad	0.43 rad
δ_a	−0.26 rad	0.26 rad
δ_r	−0.35 rad	0.35 rad
α	−0.26 rad	0.26 rad
Equilibrium flight conditions at $h = 7500$ m, Mach $= 0.6$		
$\delta_a, \delta_e, \delta_r$	0 rad	
δ_{th}	40%	
p, q, r	0 rad/s	
V	185 m/s	
α, θ	0.01 rad	
ϕ, β	0 rad	

Figure 11 shows a comparison between the reference and the achieved values of the controlled outputs when the limits described in Table 2 become active during the simulation. The aircraft exhibits a fatal loss of performance in correspondence with the pilot demand. Figures 12a–12c show the time histories of the control surface deflections. A saturation of all the actuators takes place, and the angle of attack exceeds its safety limits (Fig. 12d).

2. *Performance Achieved with CG Device*

A comparison between the original reference signal, the set points generated by the CG device, and the time histories of the controlled variables ϕ, θ, and β are shown in Fig. 13. Note that the time evolution of the new reference signals differs from the original one. Because of the CG action, the controlled outputs (solid line) exhibit good tracking properties with respect to the new reference signals. As a consequence, the aircraft holds a stable behavior with an acceptable flight performance. The control action is reported in Fig. 14; the CG device can be added to avoid input saturations and angle of attack excursions out of its safety limits.

For the SCA example, the finite time k^* computed solving the offline problem (21) is 18. Set $\mathcal{C}$ can be readily obtained from the constraints reported in Table 2, whereas set $\mathcal{D}$ is the same as for the HIRM example.

C. Overall Computational Burden

In both the proposed numerical examples, the CG procedures have been entirely implemented in the Matlab/Simulink environment so as to make easier their integration with the existing aircraft simulators.

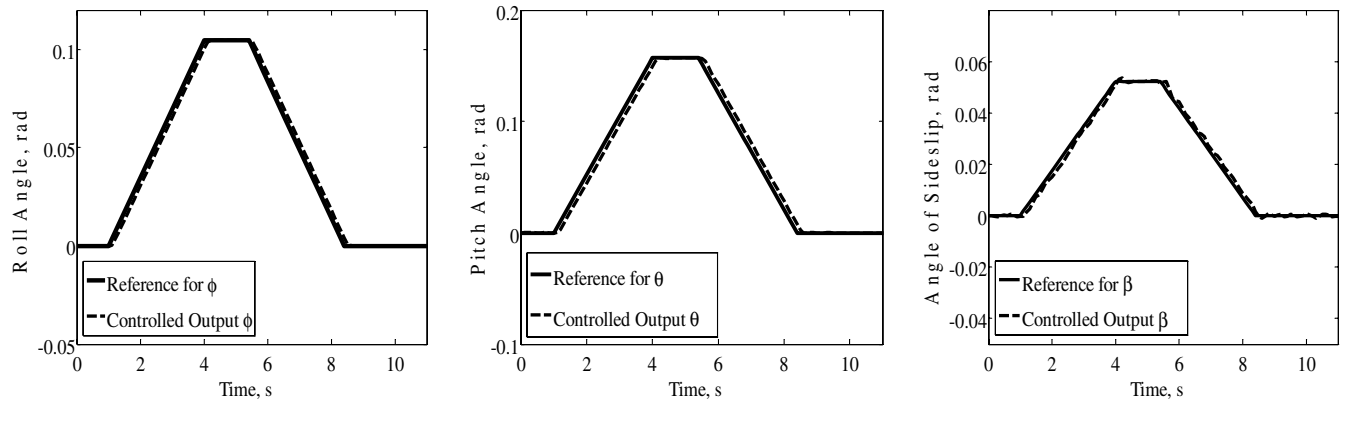

a) b) c)

Fig. 10 SCA model. Time behavior of the controlled outputs (dashed line) in the presence of a scaled reference maneuver (solid line) defined as follows: ϕ demand = 0.11 rad, θ demand = 0.16 rad, β demand = 0.05 rad (no CG action, no active constraints).

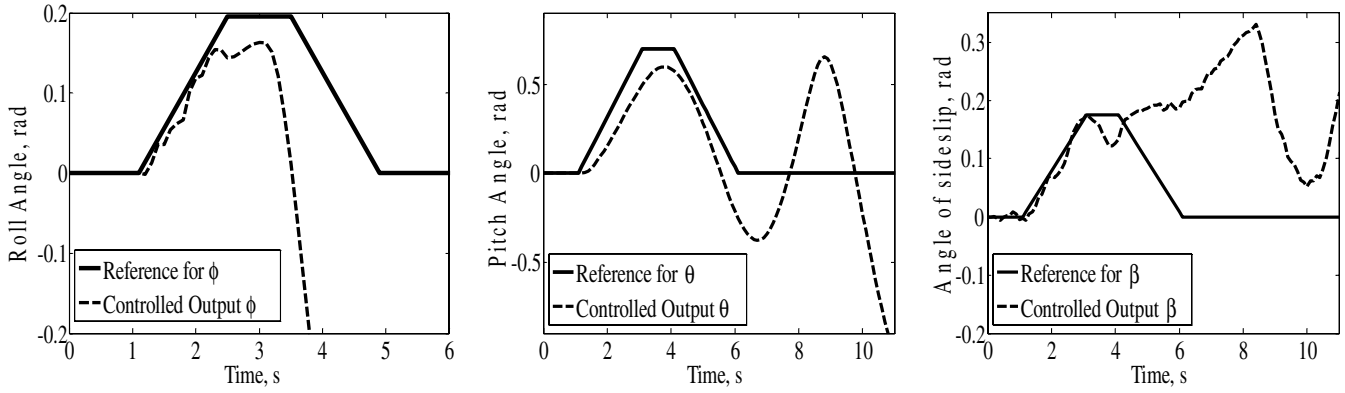

a) b) c)

Fig. 11 SCA model. Time behavior of the controlled outputs ϕ, θ, and β (dashed line) and of the pilot demands in Sec. IV.B (solid line) in the presence of constraints (no CG action).

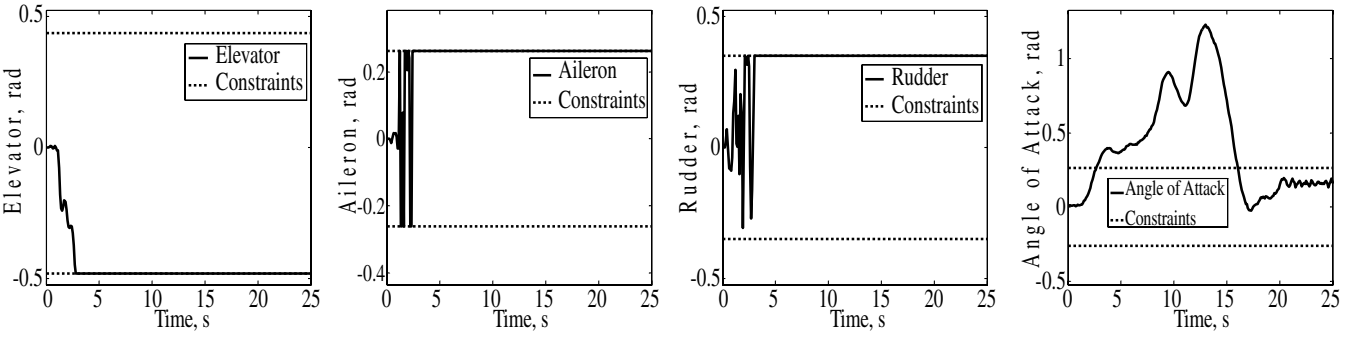

a) b) c) d)

Fig. 12 SCA model. Time behavior of δ_e, δ_a, δ_r, and α in the presence of the pilot demands in Sec. IV.B and in the presence of constraints (no CG action).

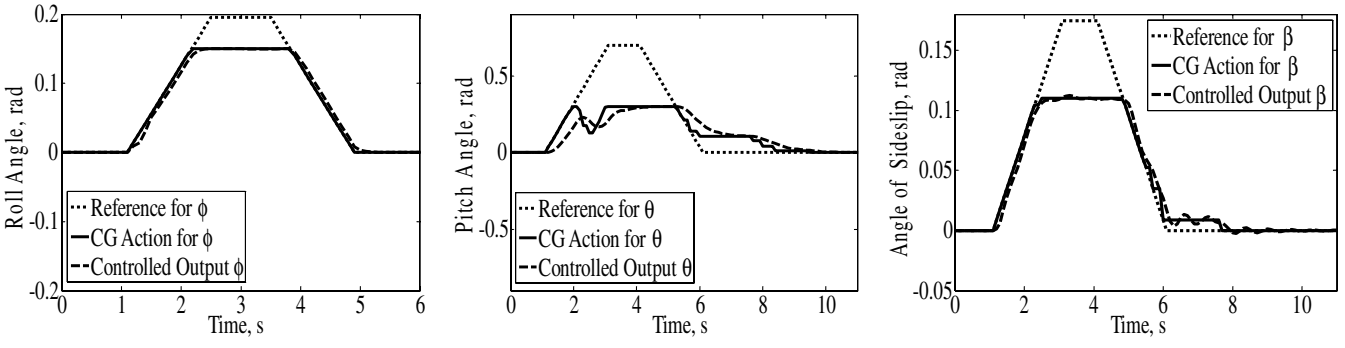

a) b) c)

Fig. 13 SCA model. Comparison between the original reference signal (dotted line), the reference signals generated by the CG (dashed line), and the time behavior of the controlled outputs (solid line).

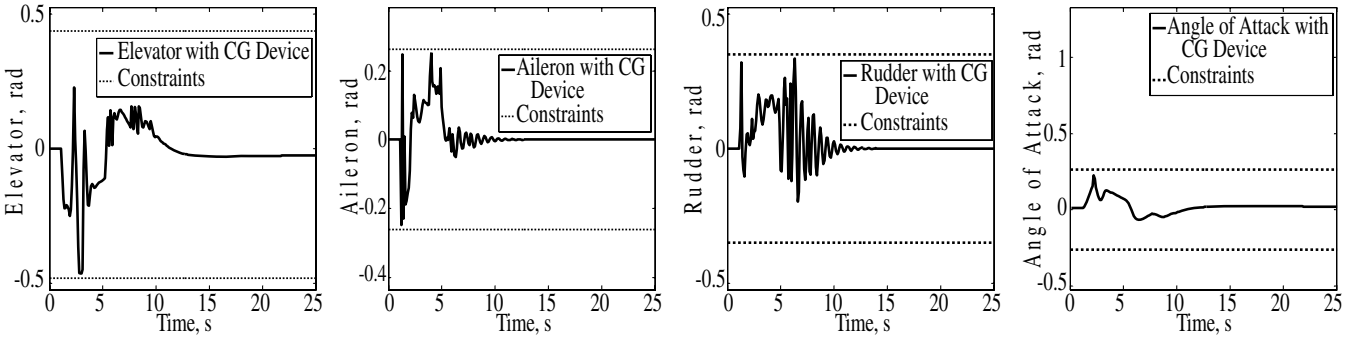

a) b) c) d)

Fig. 14 SCA model. Time behavior of δ_e, δ_a, δ_r, and α in the presence of the CG device.

Table 3 CG single step computation times (values computed in the Matlab environment with a PC with Intel Core 2 Duo technology)

	HIRM example	SCA example
T_s	100 ms	100 ms
Max. time	84 ms	79 ms
Min. time	0.14 ms	0.10 ms
Average time	17.8 ms	13.5 ms

The QP solver of the optimization toolbox has been used to solve problem (23) and the CPU-time routine has been exploited to obtain all of the the timing performance. In this respect, Table 3 shows some details on the computational load.

Although the theoretical results cannot assure that the computation time is compatible with the prescribed sampling period, it can be noted that, in both the application cases considered, the required computational burden results are acceptable. Moreover, as noted in Sec. III, in the event that, at a certain step, the current CG command is not available "in time," it can be safely recovered by applying the modified reference signal provided by the CG at the previous time step.

V. Conclusions

The presence of amplitude and/or rate saturating control effectors as well as the other limitations arising from the normal operation of aircraft is, by no means, a challenging problem for a flight control system designer. In this paper, a predictive control strategy based on the command governor approach has been investigated to solve such a problem. The main goal has been to explore the possibility of increasing the flight safety and comfort, to improve the overall control performance, and to achieve satisfactory atmospheric wind and turbulence rejection, taking into account the constraints on input and state variables. The proposed paradigm has been applied to a fighter aircraft and to a small commercial aircraft of general aviation, taken as benchmark tests. For both cases, extensive nonlinear numerical simulations, carried out in presence of a severe atmospheric turbulence scenario and fast and aggressive pilot demands, revealed a deep saturation of the allowable control effectors, a violation of the prescribed constraints, and fatal unstable aircraft behavior. It has been observed that the insertion of a command governor as an auxiliary device in the feedback loop involves a significant enhancement of the reliability and performance on both aircraft. The CG is, in fact, capable of recovering the aircraft stability in a satisfactory way by ensuring the fulfillment of all of the prescribed constraints and providing a good rejection level of the external disturbances.

The encouraging results achieved in the numerical simulation experiences suggest that the command governor strategy deserves further investigation for the application to flight control problems.

References

[1] Stevens, B. L., and Lewis, F. L., *Aircraft Control and Simulation*, 2nd ed., Wiley, Hoboken, NJ, 2003.

[2] Kothare, M. V., Campo, P. J., Morari, M., and Nett, C. N., "A Unified Framework for the Study of Anti-Windup Designs," *Automatica*, Vol. 30, No. 12, 1994, pp. 1869–1883. doi:10.1016/0005-1098(94)90048-5

[3] Avanzini, G., and Galeani, S., "Robust Antiwindup for Manual Flight Control of an Unstable Aircraft," *Journal of Guidance, Control, and Dynamics*, Vol. 28, No. 6, 2005, pp. 1275–1282. doi:10.2514/1.12004

[4] Cao, Y. Y., Lin, Z., and Ward, D. G., "H_∞ Antiwindup Design for Linear Systems Subject to Input Saturations," *Journal of Guidance, Control, and Dynamics*, Vol. 25, No. 3, 2002, pp. 455–463.

[5] Doyle, J. C., Smith, R. S., and Enns, D. F., "Control of Plants with Input Saturation Nonlinearities," *Proceedings of the American Control Conference*, Institute of Electrical and Electronics Engineers, New York, 1987, pp. 1034–1039.

[6] Teel, A. R., and Kapoor, N., "The L2-Anti-Windup Problem: Its Definition and Solution," *Proceedings of the European Control Conference*, Springer–Verlag. New York, 1997, pp. 120–128.

[7] Snell, S. A., and Hess, R. A., "Robust, Decoupled, Flight Control Design with Rate-Saturating Actuators," *Journal of Guidance, Control, and Dynamics*, Vol. 21, No. 3, 1998, pp. 361–367.

[8] Hess, R. A., and Snell, S. A., "Flight Control System Design with Rate Saturating Actuators," *Journal of Guidance, Control, and Dynamics*, Vol. 20, No. 1, 1997, pp. 90–96.

[9] Soest, W. R., Chu, P. Q., and Mulder, A., "Combined Feedback Linearization and Constrained Model Predictive Control for Entry Flight," *Journal of Guidance, Control, and Dynamics*, Vol. 29, No. 2, 2006, pp. 427–434. doi:10.2514/1.14511

[10] Menon, P. M., Bates, D. G., and Ian, P., "Computation of the Worst-Case Pilot Inputs for Nonlinear Flight Control System Analysis," *Journal of Guidance, Control, and Dynamics*, Vol. 29, No. 1, 2006, pp. 195–199. doi:10.2514/1.14687

[11] Devasia, S., and Meyer, G., "Recovery Guidance Satisfying Input and State Constraints: Rate Saturating Actuator Example," *Journal of Guidance, Control, and Dynamics*, Vol. 21, No. 5, 1998, pp. 733–741.

[12] Hennet, J. C., and Beziat, J. P., "A Class of Invariant Regulators for the Discrete-Time Linear Constrained Regulation Problems," *Automatica*, Vol. 27, No. 3, 1991, pp. 549–554. doi:10.1016/0005-1098(91)90114-H

[13] Blanchini, F., "Ultimate Boundedness Control for Uncertain Discrete-Time Systems via Set-Induced Lyapunov Functions," *IEEE Transactions on Automatic Control*, Vol. 39, No. 2, 1994, pp. 428–433. doi:10.1109/9.272351

[14] Draeger, A., Engell, S., and Ranke, H., "Model Predictive Control Using Neural Networks," *IEEE Control Systems Magazine*, Vol. 15, No. 5, Oct. 1995, pp. 61–66. doi:10.1109/37.466261

[15] Diehl, M., Bock, H. G., and Schloder, J. P., "Real-Time Iterations for Nonlinear Optimal Feedback Control," *Proceedings of the Conference on Decision and Control, and the European Control Conference*, Institute of Electrical and Electronics Engineers, New York, 2005, pp. 5871–5876.

[16] Casavola, A., Mosca, E., and Angeli, D., "Robust Command Governors for Constrained Linear Systems," *IEEE Transactions on Automatic Control*, Vol. 45, No. 11, 2000, pp. 2071–2077. doi:10.1109/9.887628

[17] Bemporad, A., Casavola, A., and Mosca, E., "Nonlinear Control of Constrained Linear Systems via Predictive Reference Management," *IEEE Transactions on Automatic Control*, Vol. 42, No. 3, 1997, pp. 340–349. doi:10.1109/9.557577

[18] Angeli, D., Casavola, A., and Mosca, E., "On Feasible Set-Membership State Estimators in Constrained Command Governor Control," *Automatica*, Vol. 37, No. 1, 2001, pp. 151–156. doi:10.1016/S0005-1098(00)00133-3

[19] Casavola, A., Mosca, E., and Papini, M., "Control Under Constraints: An Application of the Command Governor Approach to an Inverted Pendulum," *IEEE Transactions on Control Systems Technology*, Vol. 12, No. 1, 2004, pp. 193–204. doi:10.1109/TCST.2003.821953

[20] Casavola, A., and Mosca, E., "Bank-to-Turn Missile Autopilot Design via Observed-Based Command Governor Approach," *Journal of Guidance, Control, and Dynamics*, Vol. 27, No. 4, 2004, pp. 705–710. doi:10.2514/1.11163

[21] Gilbert, E. G., and Kolmanovski, I., "Fast Reference Governors for Systems with State and Control Constraints and Disturbance Inputs," *International Journal of Robust and Nonlinear Control*, Vol. 9, No. 15, 1999, pp. 1117–1141. doi:10.1002/(SICI)1099-1239(19991230)9:15<1117::AID-RNC447>3.0.CO;2-I

[22] Gilbert, E. G., and Kolmanovski, I., "Discrete-Time Reference Governors and the Nonlinear Control of Systems with State and Control Constraints," *International Journal of Robust and Nonlinear Control*, Vol. 5, No. 5, 1995, pp. 487–504. doi:10.1002/rnc.4590050508

[23] Bemporad, A., and Mosca, E., "Constraint Fulfillment in Feedback Control via Predictive Reference Management," *Proceedings of the Conference on Control Applications*, Institute of Electrical and Electronics Engineers, New York, 1994, pp. 1909–1914.

[24] Angeli, D., and Mosca, E., "Command Governors for Constrained Nonlinear Systems," *IEEE Transactions on Automatic Control*, Vol. 44, No. 4, 1999, pp. 816–820. doi:10.1109/9.754825

[25] Gilbert, E. G., and Kolmanovski, I., "Nonlinear Tracking Control in the Presence of State and Control Constraints: A Generalized Reference Governor," *Automatica*, Vol. 38, No. 12, 2002, pp. 2063–2073. doi:10.1016/S0005-1098(02)00135-8

[26] Magni, J.-F., Bennani, S., and Terlouw, J. (eds.), *Robust Flight Control: A Design Challenge*, Lecture Notes in Control and Information Sciences, Vol. 224, Springer–Verlag, Berlin, 1997.

[27] Anon., "Robust Flight Control Design Challenge Problem Formulation and Manual: the High Incidence Research Model," Group for Aeronautical Research and Technology in Europe, Rept. TP-088-4, 1996.

[28] Ferrara, F., Russo, F., Scala, S., Ciniglio, U., and Verde, L., "ADFCS Bare Aircraft Simulation Tools: Model Description and User Manual," Centro Italiano Ricerche Aerospaziali Rept. TR-98-112, 1998.

[29] Amato, F., Mattei, M., Scala, S., and Verde, L., "Robust Flight Control Design for the HIRM via Linear Quadratic Methods," *Aerospace Science and Technology*, Vol. 4, No. 6, Sept. 2000, pp. 423–438. doi:10.1016/S1270-9638(00)01067-1

[30] Mattei, M., and Scordamaglia, V., "Flight Control Design Using Multivariable PI Control with $H_2 - H_\infty$ Performance," *Proceedings of the Mediterranean Conference on Control and Automation*, Institute of Electrical and Electronics Engineers, New York, 2004, pp. 423–438.

[31] Kolmanovsky, I., and Gilbert, E. G., "Theory and Computation of Disturbance Invariant Sets for Discrete-Time Linear Systems," *Mathematical Problems in Engineering*, Vol. 4, No. 4, 1998, pp. 317–367. doi:10.1155/S1024123X98000866

[32] Kolmanovsky, I., and Gilbert, E. G., "Maximal Output Admissible Sets for Discrete-Time Systems with Disturbance Inputs," *Proceedings of the American Control Conference*, Institute of Electrical and Electronics Engineers, New York, 1996, pp. 1996–1999.

[33] Gilbert, E. G., and Tin Tan, K. L., "Linear System with State and Control Constraints: The Theory and Application of Maximal Output Admissible Sets," *IEEE Transactions on Automatic Control*, Vol. 36, No. 9, 1991, pp. 1008–1020. doi:10.1109/9.83532

[34] Angeli, D., Casavola, A., and Mosca, E., "Command Governors for Constrained Nonlinear Systems: Direct Nonlinear vs. Linearization-Based Strategies," *International Journal of Robust and Nonlinear Control*, Vol. 9, No. 10, 1999, pp. 677–699. doi:10.1002/(SICI)1099-1239(199908)9:10<677::AID-RNC424>3.0.CO;2-1

[35] Golub, G. H., and Van Loan, C. F., *Matrix Computations*, 3rd ed., The John Hopkins Univ. Press, Baltimore, MD, 1996, pp. 336–340.